A Multi-Objective VAR Planning Approach Considering Seasonal Variations of Wind Power and Solar PV

E. E. El-Araby

Department of Electrical Engineering, Faculty of Engineering, Port Said University, Egypt

(elsaid.elaraby@eng.psu.edu.eg)

Corresponding Author: E. E. El-Araby, Department of Electrical Engineering, Faculty of Engineering, Port Said University, Egypt

Tel: +20 1061460065, elsaid.elaraby@eng.psu.edu.eg

Received: 15.08.2023 Accepted:31.10.2023

Abstract- This paper proposes a stochastic multi-objective VAR planning technique that integrates seasonal variations in wind power, solar PV, and load and investigates their significant effect on the selection of VAR sources. To account for various system scenarios that could arise during the planning horizon, typical seasonal days that characterize seasonal variability associated with renewable energy sources (RES) and load are employed. The problem is described as an optimization problem with two conflicting objective functions that simultaneously yield the minimum possible investment and operating costs, as well as a sufficient VAR reserve that guarantees an appropriate security margin for all anticipated scenarios resulting from seasonal variations. The objective functions are optimized while maintaining a significant number of constraints at both the normal state and contingency situations for each hour of the typical seasonal days in the planning horizon. The problem is addressed using a hybrid strategy that combines conventional methods with the efficient multi-objective genetic algorithm NSGA-II. To demonstrate the viability of the presented methodology, it has been successfully tested on an IEEE 14-bus system.

Keywords VAR planning, wind energy, solar PV, seasonal variations, voltage security, multi-objective.

1. Introduction

Due to concerns about global warming and the rapid depletion of conventional fossil fuels, electrical power systems worldwide are undergoing a significant transition from conventional thermal generation units to renewable energy sources. Recently, several countries have set targets for integrating at least 20% of their energy production from wind and solar PV sources. The increasing penetration level of wind and PV sources brings major challenges to power system companies in the planning and operational stages due to their intrinsic uncertainty associated with unanticipated weather conditions. Recently, the reactive power planning (RPP) problem became one of the critical research topics that has been given great attention by the researchers [1-5]. It is currently undergoing a reassessment on account of the substantial degree of renewable energy penetration. The appropriate representation of the unpredictable behaviour of wind and PV sources in the long-term RPP problem is crucial to adequately assessing and quantifying the security of the power system.

The RPP problem has been investigated intensively in the literature. Its objective is to identify the optimal allocation of new reactive power resources for maintaining the voltage profile and preserving the specified voltage security margin of an expected long-term load profile [1-5]. The compromise between economic aspects "in terms of investment cost of new VAR sources as well as operating costs" and the voltage security issue is an essential task of the power system planners. The problem is very complicated in its formulation and requires special solution methodologies to achieve an acceptable compromise between cost and security. The rapid integration of large-scale RES increases the complexity of the long-term planning problem since it causes uncertain power outputs that must be precisely considered in the problem formulation. In such circumstances, a stochastic model that describes the uncertainties of the power outputs through the likely multiple scenarios is indispensable. Therefore, a reformulation of the RPP problem that considers the unpredictability of the wind and solar PV power outputs is substantially requested to simultaneously meet the appropriate voltage security limit

and the lowest overall cost. This situation has stimulated the power system planners to deal with the challenges mentioned by developing new models, as outlined below.

A considerable number of the previous studies have dealt with the RPP problem in a deterministic framework where several objective functions have been defined in the presented formulations. These objectives have been set in the form of a cost-based single objective function or multi-objective functions that include other security measures such as available transfer capability or voltage stability index besides the defined cost-based objective [1-5]. Some nondeterministic approaches have been introduced in the former studies to evaluate the effect of load and generation uncertainties on the long-term RPP problem, however, overlooking the impact of renewable energy sources [6-7].

Due to the rapid integration of large-scale renewable energy, several studies have modified the formulation of the RPP problem to represent the effect of the volatile nature of RES. The goal is to obtain the optimal VAR allocation that relieves the negative impact of the uncertain RES outputs on power system operation. Refs. [8-9] have addressed the uncertainty related to wind generation to explore its impact on long-term RPP in the distribution system grid. At the transmission systems level, wind energy has been integrated into the RPP problem without including uncertainties in some of the earlier studies [10-13]. In [10], a genetic algorithm is employed to resolve the problem of RPP in the presence of wind power, where the system loadability is maximized to find the optimal allocation of Static Var Compensators (SVCs) and wind farms. In [11], a multi-objective method is introduced for the RPP problem incorporated with wind power. The objective functions considered in the presented approach are the power losses, load power margin, and the new VAR sources' investment cost. In [12], a two-tier algorithm based on differential evolution is suggested for RPP integrated with wind energy. The objective function of the suggested method is selected to optimize power loss, the expenditures of SVCs, and the voltage profile for various penetration levels of wind power. Ref. [13] investigates the best deployment of multiple FACTS devices in deregulated systems incorporating wind generation. The presented approach considers annual net cost as an objective function that includes the annual cost of FACTS devices, operation costs, and customer benefits. A hybrid method utilizing conventional methods and particle swarm optimization is employed to resolve the problem.

At the transmission network level, a few of the previous research studies discussed the impact of renewable energy uncertainties on the RPP. The problem has been reformulated considering RES variability and presented as an optimization problem with single or multi-objective functions. Within the framework of the single objective function, Refs. [14-19] presented their proposal as a stochastic model for the RPP issue to take the uncertainties of RES into consideration. In [14], the differential evolution algorithm is employed to minimize the aggregate of the yearly cost of energy loss, the installation cost of SVC, and the system voltage deviation, which is treated as a penalty function in the objective function. The authors in [15] address the uncertainty of the wind generation in the RPP problem as Benders decomposition is utilized to solve the suggested voltage stability constrained model under the worst-case contingency. The objective function of the developed model was established to minimize predicted production costs and the investment expenses associated with VAR devices. Ref. [16] proposes a model that simultaneously minimizes a single target, including capital costs for new transmission lines, TCSC and VAR sources in addition to the costs of generation and load reduction. The load-wind scenarios were represented by a clustering method to account for the uncertainties. In [17], a stochastic model of RPP and active power dispatch considering wind load uncertainties is proposed. The objective function has been adopted to maximize the utility's annual profit, defined in terms of the cost reduction of power loss and active power generation as well as the expenses related to the added VAR sources. A multi-period, multi-scenario OPF model was presented in [18] with different demand, wind, and solar scenarios. A single cost-based goal was established in order to assess the most effective VAR investment in a certain planning period while taking into consideration the generating cost and the residual investment value. Ref. [19] extends the work introduced in [17] by proposing a probabilistic cost-based single objective function for installing new capacitor banks and SVCs, taking into consideration the unpredictable nature of wind farms, solar panels, loads, and charging for electric vehicles.

In the context of the probabilistic multi-objective RPP, few papers have been presented in the literature for the simultaneous optimization of multi-conflicting objectives, while RES uncertainties are taken into consideration [20-24]. In [20], a mixed-integer quadratic framework for RPP is presented. A multi-objective optimization model is proposed to reduce operating expenses, the load shedding threat, and the capital cost associated with the new VAR sources. The uncertainty of the load has been considered in the proposed method, while wind power uncertainty has been overlooked. Ref. [21] proposes a VAR planning tool to improve voltage resilience with the optimization of three competing objective functions. Taguchi's Orthogonal Array Testing method is employed to redesign the parameters and approximate the uncertainty region using a limited number of possibilities. Refs. [22,23] examine the probabilistic multi-objective RPP while taking load and the production of wind energy uncertainty into account. Wind power and load uncertainties were addressed using a scenario-based approach in [22], while the Information Gap Decision Theory is used in [23]. The ε-Constraint method is utilized to solve the suggested probabilistic multi-objectives, which include the minimization of investment and power loss costs as well as the maximization of loadability margin to maintain the voltage stability index. In [24], the authors suggested a multi-objective dynamic VAR device planning technique to improve voltage stability while taking wind power output uncertainty into account.

Despite the significant value of the previously mentioned studies in addressing the stochastic behaviour of the RES and load fluctuation in the RPP problem, the impact of seasonal climate changes, which have a considerable influence on the

planning decision, has been disregarded. The importance of integrating the seasonal variations of the RES and load has been realized and addressed in the long-term planning of renewable distributed generation "DG" in the distribution system in references [25–27]. As far as the authors are aware, no research studies have yet addressed the effects of including seasonal variations in load and RES in the RPP problem. It is essential to take them into account due to their substantial influence on the decision of VAR allocation, which is crucial in striking a balance between the incurred cost and system security concerns. Furthermore, the long-term RPP problem needs to be carried out while considering the relevant multi-objectives and appropriate constraints that ensure the balance between incurred costs and the required level of security, which has not been properly addressed in the preceding research. Therefore, it is necessary to present a multi-objective VAR planning formulation that considers seasonal climate variations and investigates the most appropriate model for the RES and load that captures seasonal fluctuations and their impact on the VAR planning decision.

Considering the shortcomings mentioned in the earlier studies, a multi-objective stochastic VAR planning model is introduced in this work. The following are this paper's main contributions:

1. Establishing a probabilistic multi-objective VAR planning tool that considers seasonal variations in wind power, solar PV, and load and assesses their impact on the decision of allocating VAR resources.
2. Presenting the appropriate multi-objective function formulation that simultaneously achieves the lowest cost and a sufficient VAR reserve while ensuring a predefined voltage stability margin for all potential scenarios brought on by seasonal variations.
3. Developing a hybrid solution strategy for solving the problem that takes advantage of both conventional approaches and the reliable multi-objective NSGA-II.

2. Modelling of RES and Load in the Planning Problem

Meteorological factors like solar irradiance, wind speed, and ambient temperature have a major effect on load demand as well as solar and wind power generation. This makes it extremely difficult for researchers to develop precise models of load and RES for power system planning problems that require taking into consideration their hourly fluctuations throughout the planning horizon [25-28]. Throughout the planning horizon, load and RES uncertainties can be represented using scenario-based techniques. However, 365 daily scenarios must be accounted for in the planning problem, which will necessitate a significant amount of simulation time. As a result, to lessen the computational burden, the number of daily scenarios must be decreased. In this work, this is done by dividing the year into four seasons, as the behaviour of load patterns and RES tends to be reasonably consistent throughout each season. Thereafter, a typical day is constructed for each season to illustrate the random behaviour of the load and RES. Then, each season's typical day is split into 24-time segments, each of which represents an hour of the season. Gaussian, Beta, and Weibull probability density functions (PDF) are employed to estimate the hourly load, solar irradiance, and wind speed data, respectively, as explained in the sections that follow.

2.1. Generation of a Typical Seasonal Day Scenario

In order to establish a typical seasonal day scenario for the load and RES, a year is first separated into four seasons, which stand for spring, summer, fall, and winter. Then, the data from the past years at a specific site for each season can be collected individually, where the mean value and the standard deviation of each hour of a typical day can be easily computed. For example, if the summer has N_d days and the load and RES data for the previous N_y years are available, then each hour t of a typical summer day has $N_s^t = (N_y * N_d)$ values, and the mean value μ^t and standard deviation σ^t for each hour can be computed using the following equations:

$$\mu^t = \frac{1}{N_s^t}\sum_{i=1}^{N_s^t} D_i^t \tag{1}$$

$$\sigma^t = \sqrt{\frac{1}{N_s^t}\sum_{i=1}^{N_s^t}(D_i^t - \mu^t)^2} \tag{2}$$

where N_s^t denotes the total number of data points for hour t, and D_i^t stands for the i^{th} data point for that hour.

The above values of μ^t and σ^t are so important for constructing the typical seasonal day, as they can be easily employed in the PDF of RES and load demand as follows:

2.1.1. Wind power modelling

For every hour of the typical day of the season, the stochastic behaviour of wind speed can be characterized by the Weibull PDF provided by Equation (3), [29,30].

$$f_v(v) = \frac{k}{C}\left(\frac{v}{C}\right)^{k-1}\exp\left(-\left(\frac{v}{C}\right)^k\right) \tag{3}$$

where v stands for the wind speed, C denotes the scale parameter, and k denotes the shape parameter.

The mean value and standard deviation corresponding to each hour of the typical day decided by (1) and (2) are utilized to define the shape and scale parameters using the Gamma function Γ as follows [29,30]:

$$k = \left(\frac{\sigma^t}{\mu^t}\right)^{-1.086}; \quad C = \frac{\mu^t}{\Gamma(1+1/k)} \tag{4}$$

Since we have assumed that the wind speed follows Weibull PDF, the average power of each hour might be calculated by first dividing PDF into an equal number N_i of segments, each with a mean speed v_m^i. Then, the probability $P_v(v^i)$ of a specific wind speed v^i for the specified segment *i* and its relevant power $P_w(v^i)$ would be evaluated by Equations (5) and (6), respectively. Finally, the average power of each hour can be easily estimated using Equation (7).

$$P_v(v^i = v_m^i) = \int_{v_l}^{v_n} f_v(v^i) \tag{5}$$

$$P_w(v^i) = \begin{cases} 0 & v^i \le v_{ci},\ v^i \ge v_{co} \\ p_r \dfrac{v^i - v_{ci}}{v_r - v_{ci}} & v_{ci} < v^i < v_r \\ p_r & v_r < v^i < v_{co} \end{cases} \tag{6}$$

$$P_w^t = \sum_{i=}^{N_i} P_v(v^i) * P_w(v^i) \tag{7}$$

where $v_m^i = (v_l + v_n)/2$ is the mean speed at segment i; v_{ci}, v_{co}, and v_r are the cut-in, cut-out, and rated speed of the wind turbine respectively; p_r is the rated power of the wind turbine; $P_w(v^i)$ is turbine output power at speed v^i; and P_w^t is the average wind power at hour t of the typical seasonal day.

2.2.2. Solar power modelling

The same procedures employed for modelling average wind power output are repeated for the historical data of solar irradiance to model PV average output at a specific site. The random behaviour of the solar irradiance can be described by using the Beta PDF, as has been recommended in several previous studies [29,30]. First, Equations (1) and (2) are used to calculate μ^t and σ^t for the sun irradiance for every single hour of a typical day. Then, the Beta PDF $f_s(S)$ is constructed using the following equation:

$$f_s(S) = \frac{\Gamma(\alpha+\beta)}{\Gamma\alpha\Gamma\beta} * S^{(\alpha-1)} * (1-S)^{(\beta-1)}, \quad \alpha > 0;\quad \beta > 0;\quad 0 \le S \le 1 \tag{8}$$

where S is the sun irradiance (kw/m^2); α and β represents parameters of the Beta PDF and are determined as follows:

$$\beta = (1-\mu^t) * \left(\frac{\mu^t * (1+\mu^t)}{(\sigma^t)^2} - 1\right) \tag{9}$$

$$\alpha = \frac{\mu^t * \beta}{1-\mu^t} \tag{10}$$

To compute the average power of each hour in this case, the PDF given by (8) is divided into a number of equal segments N_j each with a mean solar irradiance S_m^j. Then, the probability $P_s(S^j)$ of specific S^j for the specified segment j and its relevant power $P_{pv}(S^j)$ would be evaluated by Equations (11) and (12), respectively. Finally, the average power of each hour can be easily estimated using Equation (13).

$$P_s(S^j = S_m^j) = \int_{S_l}^{S_n} f_s(S^j) \tag{11}$$

$$P_{pv}(S^j) = N_{pv} * FF * V_{pv}^j * I_{pv}^j \tag{12}$$

$$P_{pv}^t = \sum_{j=1}^{N_j} P_s(S^j) * P_{pv}(S^j) \tag{13}$$

where $S_m^j = (S_l + S_n)/2$ is the mean solar irradiance at segment j; N_{pv} is the total number of PV modules; FF stands for fill factor; V_{pv}^j and I_{pv}^j are the voltage and current of PV module at state *j*; $P_{pv}(S^j)$ is the PV array's power generation at solar irradiance S^j, and P_{pv}^t is the PV array's hourly average power production correlated to hour *t* of the typical seasonal day.

The current I_{pv}^j and voltage V_{pv}^j of a PV module for a particular irradiance S_m^j, cell temperature T_C^j, and the fill factor FF can be determined using the following equations [25].

$$T_C^j = T_A + S_m^j * \left(\frac{N_{OT} - 20}{0.8}\right) \tag{14}$$

$$I_{pv}^j = S_m^j [I_{SC} + K_i (T_C^j - 25)] \tag{15}$$

$$V_{pv}^j = V_{OC} - K_v * T_C^j \tag{16}$$

$$FF = \frac{V_{MPP} * I_{MPP}}{V_{OC} * I_{SC}} \tag{17}$$

where T_A and N_{OT} are the ambient temperature and normal operating temperature, respectively; K_i and K_v are the current and voltage temperature coefficients; I_{SC} and V_{OC} are the PV module's open circuit voltage and short circuit current, respectively; I_{MPP}, V_{MPP} are the current and voltage at the maximum power point.

2.2.3. Load modelling

Based on the mean value and standard deviation relevant to each hour of the typical seasonal day, a Gaussian distribution can be used to describe the variation of load demand over a particular hour. The Gaussian distribution is then discretized into a number of stats N_g, where the

probability of the load corresponding to each state g can be readily estimated by the following equation [29,30]:

$$f_g(D^g) = \frac{1}{\sigma^t\sqrt{2\pi}} \exp - \frac{1}{2}\left(\frac{D^g - \mu^t}{\sigma^t}\right)^2 \quad (18)$$

where D^g is the load demand for state g and f_g is the probability of state g.

Finally, the average load demand P_D^t of each hour of the typical day is evaluated by using Equation (19) given below.

$$P_D^t = \sum_{g=1}^{N_g} f_g(D^g) * D^g \quad (19)$$

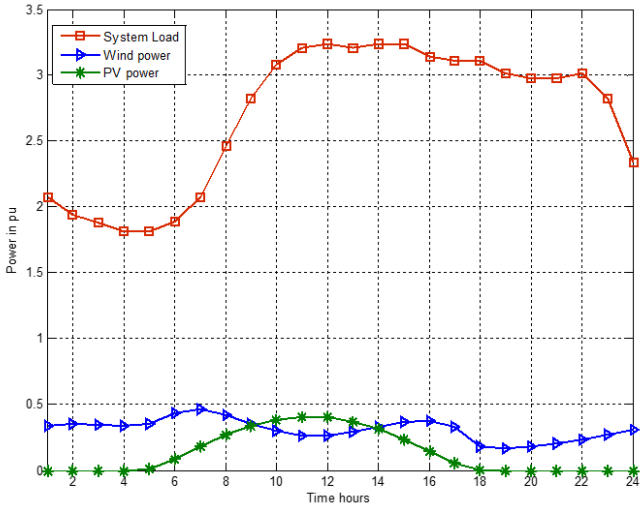

Fig. 1. RES power and load for a typical summer day.

3. Problem Formulation

This section introduces the developed probabilistic approach for the long-term RPP problem that simultaneously optimizes multi-objective functions, such as investment cost, operating cost, and system performance, in terms of voltage security and VAR reserve margin in both the normal and contingency states. The basic principle underlying the suggested method is to incorporate the probabilistic generation and load models within the standard deterministic optimization equations. As previously noted, once the average power of the PV and wind farms as well as the average load are estimated for each hour, the average power and load for a typical day in each season can be simply produced. An illustration of a typical seasonal day that might be generated throughout the summer is shown in Fig. 1. There are 24 scenarios created for each of the four seasons, so 96 will be built for an entire year. The proposed formulation is constructed so that all 96 possibilities of the year will be deterministically accommodated. The objective functions of the proposed probabilistic multi-objective technique might be described by the following equation:

$$\begin{aligned} &Min\ \ F_T = F_{IT} + F_{op} \quad \& \quad Max\ F_{res}; \\ &where, \quad F_{op} = F_l + F_c \end{aligned} \quad (20)$$

where F_{IT} is the total VAR investment cost; F_{op} is the annual operating cost; F_l is cost of energy losses; F_c is the control cost; and F_{res} is the generators' reactive power reserve.

The following subsections provide a detailed explanation of each objective function and its related constraints.

3.1. Investment Cost and Constraints

In this paper, SVCs are chosen as the new VAR devices to be installed. The installation cost of new SVC devices and associated constraints are expressed as given by Equations (21) to (24). More details on these equations are provided in [31].

$$F_{It} = \frac{i_{nt}(1+i_{nt})^{Dp}}{(1+i_{nt})^{Dp} - 1} F_{It0} \quad (21)$$

$$F_{It0} = \sum_{i=\Omega} \mu_{isvc} c_{isvc} \quad (22)$$

$$\mu_{isvc} = 0.0003 c_{isvc}^2 - 0.3051 c_{isvc} + 127.38 \quad (23)$$

$$0 \le c_{isvc} \le c_{isvc\max} \quad for\ i \in \Omega \quad (24)$$

where F_{It0} is the installation cost for the new SVCs; Ω is the set of all potential buses; μ_{isvc} is the cost for SVC in \$/KVAR; c_{isvc} is the installed SVC's size in MVAR; $c_{isvc\max}$ is the maximum capacity of the SVC devices, F_{It} is the annual investment cost; i_{nt} and Dp are the yearly interest rate and SVC's life span, respectively.

3.2. Annual Operating Cost

The operating annual cost considered in this study under a specific load growth expectation for the selected planning horizon is a strategy for reducing the sum of two key costs: total energy losses and control costs. These annual operating costs are described in further detail below:

3.2.1. Annual energy losses cost

Minimizing annual energy losses for the prospective states associated with the typical day of each season is one of the key goals of the planning formulation. Since 96 potential states are taken into account for each year, as was already explained, the objective function of the annual energy cost is as follows:

$$Min\ F_l = \sum_{N=1}^{Dy} \sum_{Ns=1}^{4} \sum_{Hr=1}^{24} P_{loss}(N, Ns, Hr) * (8760/96) * \rho * K_{re\cov} \quad (25)$$

where P_{loss} is the power losses; ρ is the energy price (\$/MW-h); and $K_{re\cov}$ is the recovery factor converting the total energy of the planning horizon into a uniform annual energy.

3.2.2. Annual control cost

In the event of a serious contingency, it is assumed that the quick corrective control will be employed to restore the system. The cost function for corrective control includes control costs for fast VAR controllers, which are the SVC devices and generators, as well as the final alternative of load shedding that will be imposed by the system operators. The chosen annual corrective control cost is represented by the following Equation [32]:

$$Min\ F_c = \sum_{N=1}^{Dy}\sum_{Ns=1}^{4}\sum_{Hr=1}^{24} F_{cc}(N,Ns,Hr)*(8760/96)*K_{re\,\mathrm{cov}}$$

$$F_{cc} = \sum_{k=1}^{ns} F_{cc}^{n}$$

$$F_{cc}^{n} = \sum_{gi=1}^{ng}\mu_{gi}\left|Q_{gi}^{(c,n)} - Q_{gi}^{0}\right| + \sum_{m=1}^{mf}\mu_{m}\left|C_{m}^{(c,n)} - C_{m}^{0}\right| + \sum_{ish=1}^{nsh}\mu_{ish}Lish \quad \text{.....(26)}$$

where subscripts *0* and c refer to the base case and contingency states ; $k=(1,2\ldots,ns)$ represents contingency number; F_{cc} is the corrective control cost, Q_g is the VAR output of generator *g*, and C_m is the VAR associated with the SVC device m. *Lish* is the load shedding of participant ish required by the system operator.

3.3 Objective Function of VAR Reserve

Maintaining enough reactive power reserve from generator VAR sources that can be quickly used in emergency situations is important to ensure the reliable operation of modern power systems, especially in critical situations like severe faults. This will protect the system from voltage instability that might be brought on by significant contingencies. One of the intrinsic functions of the power system operators is to maximize the VAR reserve for appropriate corrective control actions to protect the security of the system because they are responsible for enhancing system performance against extreme emergencies. Therefore, in this paper, the objective function described by Equation (27) of maximizing VAR reserve from the generators is selected to quantify the security measure of the system. For further details regarding Equation (27), see [32].

$$Max\ F_{res} = Min\left\{ Min\sum_{n=1}^{ns}\frac{1}{\sum_{gi=1}^{ng}\left|pf_{gi}^{n}*(Q_{gi}^{n*} - Q_{gi}^{b})\right|}\ \text{(for 96 states)}\right\}$$

……(27)

where Q_g^b is generator VAR at base case; Q_{gi}^{n*} is the generator VAR produced under contingency n at the nose point; pf_{gi}^{n} is the participation factor of generator g_i for contingency n, and ng is the number of the generators.

It should be highlighted that since F_{res} in Equation (27) is estimated for the 96 states of the four seasons, the lowest VAR reserve among the 96 values is chosen to reflect the system security measure as a conservative quantity.

3.4. Operating Constraints

The operating constraints consist of a set of constraints for each of the 96 states associated with the typical day of the four seasons described in Section 2. Two sets of constraints are established for each of the 96 states to preserve the load power margin associated with every state: the normal operating point constraints (28) and the nose point constraints (29). The authors' earlier work [1] presents the details of Equations (28) and (29). The next set of operational constraints is employed for base case 0 and each contingency *k*.

$$\left.\begin{aligned} & y_b^t - f(x_b^t, u_b^t, ci_b^t) = 0 \\ & x_{\min} \le x_b^t \le x_{\max}, \\ & u_{\min} \le u_b^t \le u_{\max},\ 0 \le ci_b^t \le c_{isvc}, \\ & 0 \le Lish_b^t \le Lish_{\max}^t \end{aligned}\right\}, \begin{pmatrix} \text{t=1,2,...,96} \\ \text{k1=0,1,2,...,ns} \end{pmatrix}$$

…….....(28)

$$\left.\begin{aligned} & y_b^t + (\lambda_c^t - 1)y_d - f(x_c^t, u_c^{(t}, ci_c^t) = 0 \\ & w(x_c^t, u_c^t, \lambda_c^t, ci_c^t)\, f_x(x_c^t, u_c^t, \lambda_c^t, ci_c^t) = 0,\ \ \|w\| \ne 0 \\ & \mathrm{u}_{\min} \le u_c^t \le u_{\max},\ \ \lambda_c^t \le \lambda_{\min},\ \ 0 \le ci_c^t \le c_{isvc}, \\ & 0 \le Lish_c^t \le Lish_{\max}^t \end{aligned}\right\}, \begin{pmatrix} \text{t=1,2,...,96} \\ \text{k1=0,1,2,..,ns} \end{pmatrix}$$

…….....(29)

where subscripts *b* and *c* denote the normal operating point and the nose point (voltage collapse point), respectively. k1= (0,1,2…, ns) indicates the base case and simulated contingencies. y_b is the power flow mismatch vector *"*including the outputs of wind and solar farms" at the normal operating point. f stands for the equations of power flow at the normal operating point. w is the left eigenvector. f_x is the power flow Jacobian. y_d is a vector of load direction. λ is the load power margin. x is the vector of state parameters. u is a set of control vector for VAR devices that already exist. ci is the new SVCs' control variable.

It is important to note that the constraints of load flow (28-29) consider the effect of the wind farm and PV outputs by adding their values to the mismatch vector y_b^t. Furthermore, bear in mind that the system operator might employ load shedding *Lish* in an emergency as a last resort.

4. Proposed Solution Method

One of the main challenges in solving the optimization model presented is that it is expressed as a large-scale non-linear programming problem because 96 possible states of a typical seasonal day are taken into account for each year of the planning horizon, in addition to the contingency states and their associated operating constraints. The conventional approaches can encounter challenges and lose their potential to provide the most viable solution, so they cannot be directly applied as standard solution techniques for this problem type. An additional challenge is that the suggested approach addresses a problem with generalized multi-objective optimization with two conflicting objective functions. The first objective is to minimize the overall cost of the VAR investment cost (F_{IT}) and yearly operating cost (F_{op}), and the second objective is to maximize VAR reserve (F_{res}) of the generators. Instead of producing only one solution for a single-objective optimization problem, a MOF can generate a series of trade-off solutions known as Pareto optimal solutions based on the dominance concept. For a solution to be deemed a Pareto solution, it is unlikely to enhance one objective function without degrading the others. This collection of solutions is referred to as the Pareto front. Among the Pareto-front solutions, the decision-makers choose one of them based on which is more efficient and effective. This paper presents a hybrid approach to solving problems that takes advantage of both conventional approaches and the robust NSGA-II algorithm to find the Pareto Front. The detailed explanation of NSGA-II algorithm can be found in [33-34].

The proposed technique to solve the problem arises from the observation that the formulation given above lacks dynamic coupling. The above-mentioned model can be written as a series of separate OPF problems that might be addressed independently for each hour by dividing it into hourly sub-problems.

Fig. 2 displays the main flowchart of the proposed methodology. The following is the computation procedure for the proposed hybrid solution technique in Fig. 2, which combines NSGA-II with traditional optimization method:

Step 1: Establish the typical seasonal day for each year of the specified planning horizon using the system data, starting with the first year.

Step 2: Generate an initial population at random (Candidate 1, Candidate 2,……. Candidate n), with each individual representing a potential solution.

Step 3: For each individual, do the following:

3.1 *Evaluate the annual investment cost* F_{IT} *using (21-24)*

3.2 *Solve (25-29) separately for each hour of each season using the conventional approach. Then, for each hour i of the 96 hours being addressed, find* F_{op}^{i} *and* F_{res}^{i}.

3.3 *For year 1, find the operating cost and the maximum VAR reserve using the following equation:*

$$F_{op}^{y1} = \sum_{i=1}^{96} F_{op}^{i} \;\&\; F_{res}^{y1} = \max(F_{res}^{i}),\ i = 1...96$$

Step 4: Repeat ***step 3*** for each year of the planning horizon. Then, determine the maximum VAR reserve of all the examined scenarios as well as the overall operating cost of the planning years. The lowest VAR reserve among all possible scenarios is selected as a conservative quantity, as pointed out before.

Step 5: Evaluate and assign a fitness value for each candidate of the current population.

Step 6: Rank the potential solutions in the Pareto front according to their levels of non-dominancy.

Step 7: The new generation of candidate solutions, often referred to as offspring, is generated using the traditional GA operators, namely mutation, recombination, and crossover.

Step 8: If the termination requirement is met, stop. Otherwise, the computation process will return to ***step 3***.

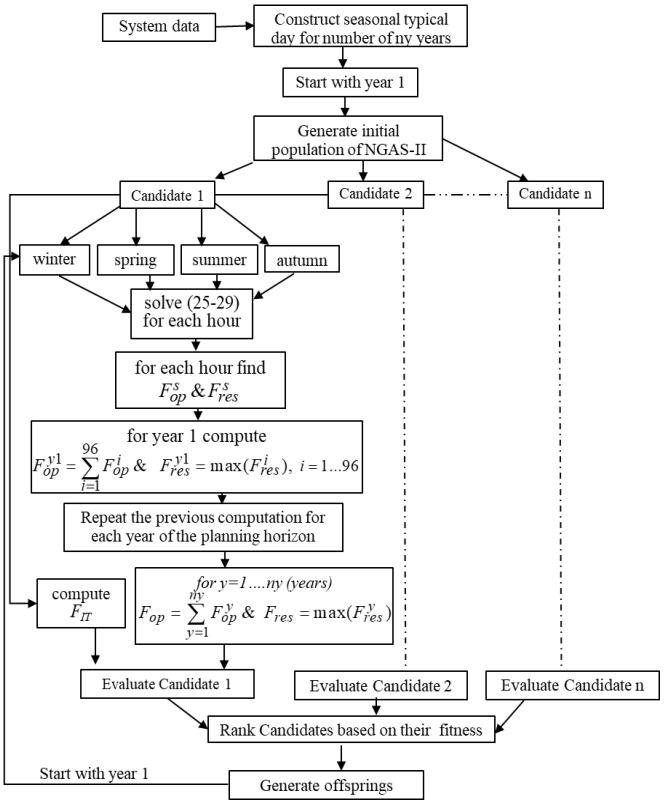

Fig. 2. Proposed solution algorithm.

A key factor in the above solution procedures is the representation of the decision variables in each individual of the population. In this work, an individual is modelled with two parts, the left part of which corresponds to the sizes of the new SVCs within the constraints set by (24), and the right part of which represents the generators' maximum VAR to be employed at the base case for each investigated scenario, as illustrated in Fig. 3. As stated in the third step of the solution procedures, every individual will be assessed using Equations (21-24) and (25-29) and will be a common candidate solution for all transition states. It should be noted

that the maximum VAR $Q^b_{g\max i}$ that can be produced is limited by the VAR capability limit $Q^{cap}_{g\max i}$ of each generator and is only employed in the generator's VAR production mode. This is because producing VAR plays a crucial role in ensuring the voltage stability margin in the examined transition states. Please refer to [32] for further details regarding the generators' VAR representation in the VAR reserve problem.

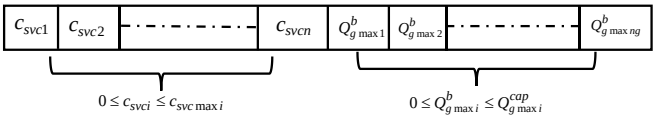

Fig.3. Individual representation

5. Simulation Results

The proposed method was implemented in the IEEE-14 bus test system to evaluate its effectiveness and validity. The simulations were conducted in the MATLAB platform using a PC with an Intel Core i7-7500U CPU, 2.7 GHz, and 8 GB RAM. The original system has been modified to include a wind farm at bus number five and a solar power plant at bus number fourteen. The maximum installed capacities of the wind farm and the solar power plant are estimated to be 100 MW and 60 MW, respectively. The technical parameters of the employed wind turbine and PV module are provided in [26]. In this study, the hourly historical data for the sun irradiance and wind speed at Ras Gharib, Egypt, are gathered from DATA.NASA.GOV data sets [36]. Hence, the year is split into the four seasons of summer (July to September), fall (October to December), winter (January to March), and spring (April to June). Every single season is exemplified by 24 segments, each of which refers to a specific hour of the full season. Hence, over the entire year, there are 96 hours (24 for each season). The mean and standard deviation of wind speed and solar irradiance are calculated for each hour using previous data collected at the site, and as a result, the pertinent hourly Weibull and Beta PDFs are produced. After that, to determine the hourly average power, the hourly Weibull and Beta PDFs are split up into a number of segments, each of which has its own probability. Finally, using Equations (7) and (13), the hourly average power for the wind farm and PV is determined. In this study, 25 and 20 discrete segments are used for the Weibull and Beta PDFs, respectively. In a similar manner, the hourly average load in a typical seasonal day can be computed by employing a Gaussian distribution for the hourly load and subsequently using Equation (18). Due to the lack of load data, it is assumed in this work that the daily load profile will match the load profile of the typical seasonal day presented in the IEEE-RTS [25] system, where the hourly load of the typical seasonal day is specified in proportion to the annual peak demand. The typical seasonal days that have been generated throughout the various seasons and employed in the subsequent simulation of the VAR planning problem are depicted in figures 1, 4, 5, and 6.

As the first step of the computational tasks, the original seasonal load has been increased by a defined load growth for the designated planning period. Then, the security limits in terms of voltage level and load margin have been examined to demonstrate the essential requirements of installing new SVCs to enhance system security. In this study, it is assumed that the load growth rate, SVC device life span (Dp), and interest rate (i_{nt}) are 3%, 10 years, and 4%, respectively. The lowest bus voltages and load power margins for the base case and immediately following the most serious contingency are shown in Table 1 for each season. As can be observed in Table 1, due to the relatively high load level of the summer season, the system has encountered extremely low load margin values and bus voltage magnitudes that go beyond predefined limits. Furthermore, in contrast to the fall and spring seasons, which have a relatively low load level and where the security limits are kept in both the base case and contingency states, during the winter season the security limits of voltage magnitudes and load margin have been slightly violated in the contingency state. In the present investigation, it is assumed that the security limits maintain bus voltages between 0.9 and 1.1 pu and a load power margin larger than or equal to 0.20. To evaluate the effectiveness of the developed method in keeping prescribed system security at a minimum cost on the planning horizon, the subsequent two cases have been investigated. The following control cost parameters were applied in this simulation [31,32]:

$\mu_{ish} = 124000$ \$/Mw, $\rho = 100$ \$/Mw-h, $\mu_{gi} = \mu_m = 1$ \$/MVArh

Table 1. Minimum bus voltage and load margin for a typical seasonal day

State		Fall	Winter	Summer	Spring
Base Case	v_{min}	0.95	0.91	0.80	0.93
	λ	0.28	0.24	0.12	0.26
Contingency	v_{min}	0.92	0.88	0.77	0.91
	λ	0.23	0.18	0.06	0.22

For NSGA-II, the maximum number of iterations and population size are 50 and 100, respectively. The probabilities of crossover and mutation are 0.8 and 0.02, respectively. Thirteen decision variables, consisting of four generator reactive power generators and nine SVCs installed at the system's load buses, form each individual in the population.

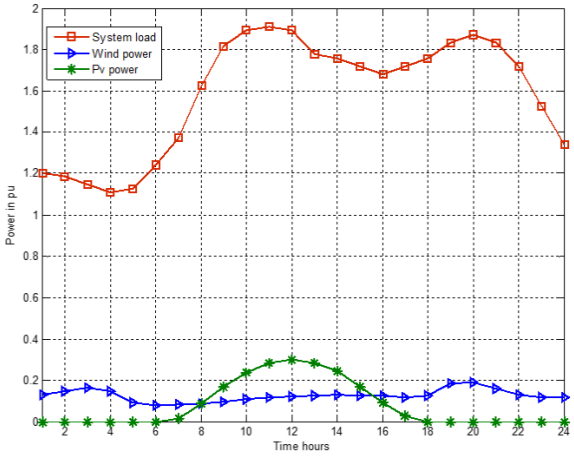

Fig. 4. RES power and load for a typical fall day.

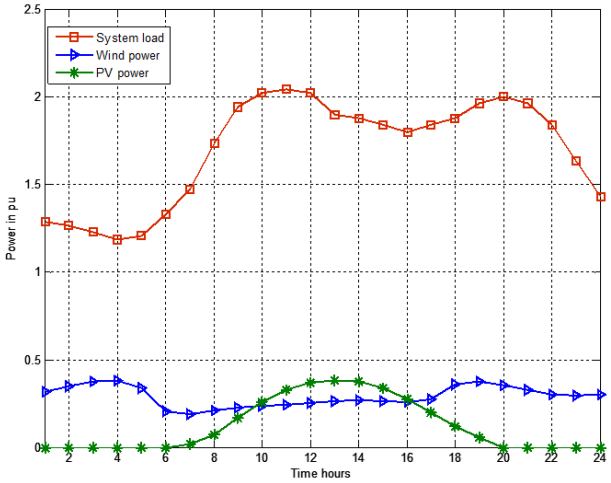

Fig. 5. RES power and load for a typical spring day.

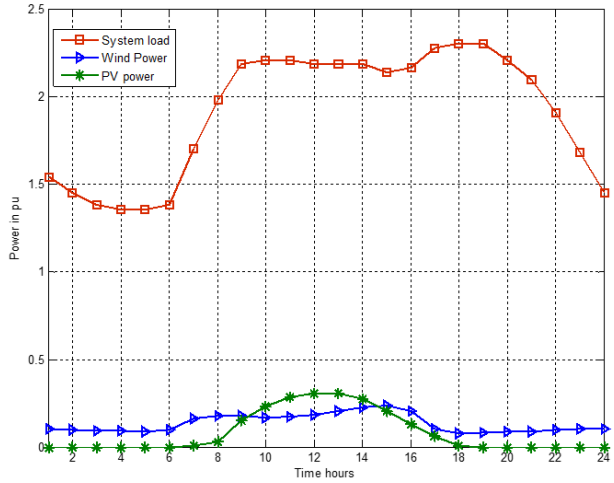

Fig. 6. RES power and load for a typical winter day.

Case 1: Without SVCs Expansion

In this examination, there is no SVCs expansion plan where load shedding is employed to obtain the Pareto optimal solutions to the proposed multi-objective problem. The planning is carried out for four typical seasonal days, as indicated by Figures 1, 4, 5, and 6. Table 2 provides the results for the total generators' VAR reserve and VAR output of each generator, relevant to the lowest and highest costs. As illustrated in the table, the minimal cost is acquired when the VAR reserve is at its lowest point, and the most cost is incurred when the VAR reserve is at its highest point. Be aware that the generators' Var outputs in the base case are somewhat higher at the imposed minimum cost than at the incurred maximum cost, resulting in a minimal reserve at the minimum cost and vice versa at the maximum. The remaining solutions (between least cost and maximum cost) can be easily identified from the Pareto optimal solutions of the simulation.

Case 2: With SVCs Expansion

In this investigation, the new SVCs are supposed to be optimally acquired to meet the security criteria of maintaining bus voltages and load margins within the established limits and maintaining a sufficient VAR reserve. Three scenarios have been evaluated to confirm how the representation of the four typical seasonal days for the year can influence the optimal solution of the problem. The three scenarios represent the planning decision (with installing new SVCs) when we assess the system under maximum load at each hour of a typical summer day, merely a typical summer day as shown in Fig. 1, and finally four typical seasonal days as indicated by figures 1, 4, 5, and 6. All the load buses of the IEEE 14-bus system are considered candidates for installing new SVCs with a maximum 0.3 pu. The objective of conducting the programme of the proposed formulation is to choose the most cost-effective SVCs allocation in terms of sites and sizes to maintain the prior security standards. The system planners will have access to the Pareto optimum front for each scenario, allowing them to decide which option best meets their requirements.

Table 2. Total cost and VAR reserve without SVCs

Case	Total Cost 10^8	VAR Reserve	Generators' VAR output			
			G1	G2	G3	G4
Min. cost	1.656	0.3860	0.409	0.399	0.335	0.271
Max. cost	1.947	0.6170	0.403	0.306	0.272	0.202

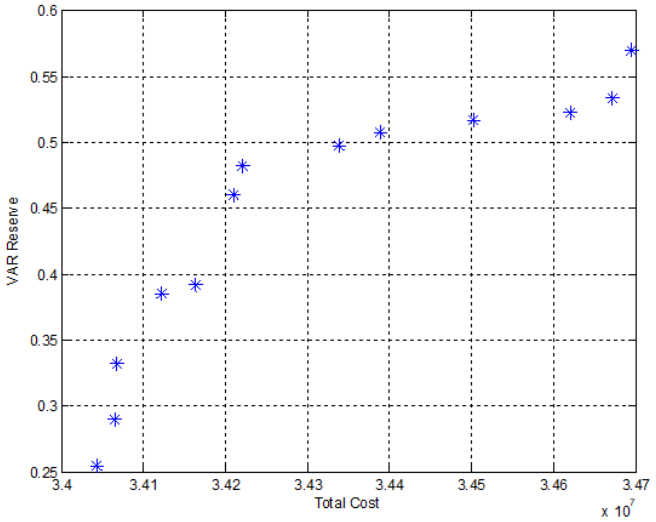

Fig. 7. Optimal Pareto front of Case 2-Scneraio

Figure 7 shows the Pareto optimum front for scenario 1, where the planning is carried out under the assumption that the summer day's maximum load will remain constant throughout the entire day. This scenario is considered the most conservative for system planners. Tables 3 and 4 give the optimal total generators' VAR reserve and SVCs allocation obtained in this analysis. Table 3 presents the results for each generator's VAR output and the total generators' VAR reserve related to the lowest and highest costs, and Table 4 shows the SVCs allocation associated with the same costs. Table 3 demonstrates that the VAR reserve for the lowest cost is less than the greatest cost. This is because the optimal SVC installation for the lowest cost is

four at buses 10, 11, 12, and 14 with a relatively low VAR amount, whereas the optimal installation for the highest cost is five SVCs at buses 5, 7, 9, 12, and 14 with larger installed values compared to the optimal installation for the lowest cost case. The overall VAR reserve is bigger at the highest cost than it is at the lowest cost due to the generators' ability to limit their VAR outputs at the base case when there is more VAR output from the installed SVCs.

Table 3. Total cost and VAR reserve (Case 2-Scneraio 1)

Case	Total Cost 10^7	VAR Reserve	Generators' VAR output			
			G1	G2	G3	G4
Min. cost	3.404	0.255	0.49	0.48	0.31	0.26
Max. cost	3.469	0.570	0.38	0.31	0.29	0.25

Table 4. Optimal VAR allocation (Case 2-Scneraio 1)

Case	SVC bus number and VAR value								
	4	5	7	9	10	11	12	13	14
Min. cost	0.0	0.0	0.0	0.0	0.14	0.14	0.11	0.13	0.0
Max. cost	0.0	0.21	0.19	0.20	0.0	0.0	0.23	0.21	0.0

The Pareto optimum front for scenario 2, when planning is done solely under the conditions of the typical summer day depicted in Fig. 1, is illustrated in Fig. 8. The results for the VAR output of each generator and the overall generators' VAR reserve, as they relate to the lowest and greatest costs, are shown in Table 5. The associated SVCs to be installed at the minimum and maximum costs are indicated in Table 6. This scenario leads to the same conclusions as scenario 1, where the lowest reserve is acquired at the lowest cost and the highest reserve is obtained at the highest cost. Additionally, the generators' VAR output at the greatest cost is comparatively lower than the lowest cost case. This is because there are more SCVs installed at the highest cost, as shown in Table 6, compared to the lowest cost. As indicated in Table 6, two SVCs are installed at buses 7 and 10 for the lowest cost scenario, while at the maximum cost case, five SVCs are installed with higher VAR sizes compared with the minimum cost case. Here, it's worthwhile to note that scenario 2's associated overall cost is cheaper than scenario 1's for the same level of VAR reserve. This is because the load during several hours of a typical summer day is lower than the maximum load employed for the entire day in scenario 1 (conservative case), and as a result, scenario 2's operating costs, including those associated with energy loss, and load shedding, are lower. This results in a lower cost for the same VAR reserve. For instance, if the VAR reserve level is equal to 0.5 pu, scenario 1's total cost would be 3.434 x $10^{\wedge 7}$, whereas scenario 2's total cost would be 2.914 x $10^{\wedge 7}$. This demonstrates how crucial it is to consider the load's variation during the entire day in order to lower the overall cost.

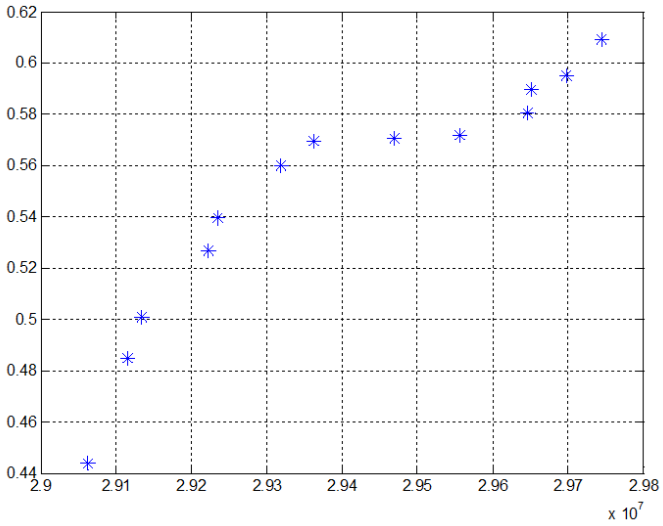

Fig. 8. Optimal Pareto front of Case 2-Scneraio 2.

Table 5. Total cost and VAR reserve (Case 2-Scneraio 2)

Case	Total Cost 10^7	VAR Reserve	Generators' VAR output			
			G1	G2	G3	G4
Min. cost	2.906	0.444	0.46	0.37	0.26	0.26
Max. cost	2.974	0.609	0.40	0.31	0.24	0.25

Table 6. Optimal VAR allocation (Case 2-Scneraio 2)

Case	SVC bus number and VAR value								
	4	5	7	9	10	11	12	13	14
Min. cost	0.0	0.0	0.13	0.0	0.28	0.0	0.0	0.0	0.0
Max. cost	0.0	0.0	0.19	0.17	0.27	0.18	0.11	0.0	0.0

At last, scenario 3 (four typical seasonal days) is examined in the case of installing new SVCs. The results of simulating this scenario are shown in Fig. 9 as well as tables 7 and 8. A significant finding is that, when compared to all previously explored scenarios, the lowest cost is achieved for the same level of the VAR reserve, as shown in Fig. 9, and Table 7. For example, the associated costs for scenarios 1, 2, and 3 for the same value of the VAR reserve, which is 0.57 pu for the three scenarios in Case 2, are 3.47x$10^{\wedge 7}$, 2.94x$10^{\wedge 7}$, and 1.48x$10^{\wedge 7}$, respectively. This shows that scenario 3 provides the best solution among the three scenarios. This is because the typical load levels in winter, fall, and spring are lower than those in summer, and as a result, this scenario's operating costs are the lowest of the

three scenarios that were analysed. This outcome clearly shows the importance of representing the four typical seasonal days for achieving the balance between economic benefit and level of security in terms of adequate VAR reserve, voltage limits, and a defined load margin. Note that Table 8 lists the SVCs combinations together with the corresponding VAR values for both the minimum and maximum cost options. These answers correspond to SVCs that were obtained at the first and last points on the optimal Prato front depicted in Fig. 9. As shown in Table 8, two SVCs are installed at buses 5 and 14 with VAR values of 0.14 and 0.17 pu, respectively, for the minimum cost and VAR reserve (first point), as opposed to the maximum cost and VAR reserve (last point), where five SVCs are installed at buses 7, 9, 11, 13, and 14 with VAR values of 0.13, 0.11, 0.10, 0.17, and 0.17 pu, respectively. The Prato front depicted in Fig. 9 presents a set of optimal options rather than just one to facilitate decision-making. The system planner can then decide which of the Pareto fronts offers the optimal compromise by using some fuzzy rules.

Finally, the cost associated with the VAR reserve of 0.617 pu in Table 2 of Case 1 (without VAR expansion) has been compared with the cost associated with the same level of VAR reserve in Case 2 of scenario 3 (with VAR expansion). In contrast to Case 1, where the cost is 1.947 x $10^{\wedge 8}$, Case 2 scenario 3 has a very low cost of 1.51 x $10^{\wedge 7}$. These findings highlight the significance of SVCs planning in enhancing system performance at a significantly lower cost as opposed to depending on the extremely expensive load shedding scenario.

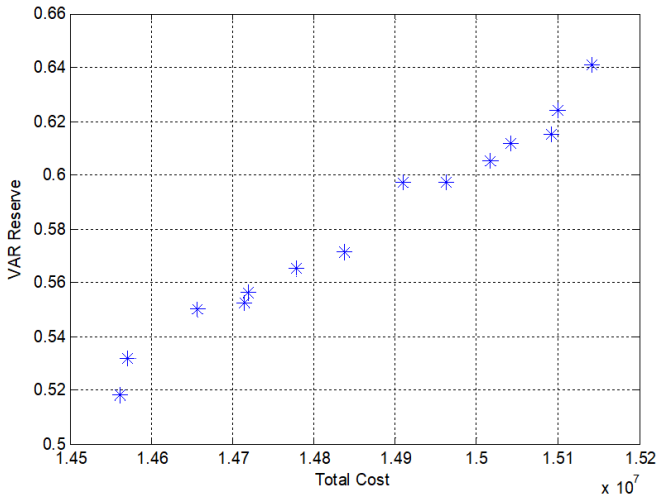

Fig. 9. Optimal Pareto front of Case 2-Scneraio 3.

It is important to highlight that even though the representation of a typical seasonal day significantly influences the best solution and yields the lowest cost, it has a heavy computational burden. The computational burdens are caused by the modelling of a substantial number of scenarios that must be taken into account for each year of the planning horizon, as well as the inclusion of a considerable number of constraints corresponding to the base cases and contingency situations. Therefore, currently, efforts are being made to simplify the formulation and make the necessary modifications to the solution technique to make the proposed approach feasible for very large systems.

Table 7. Total cost and VAR reserve (Case 2-Scneraio 3)

Case	Total Cost 10^7	VAR Reserve pu	Generators' VAR output			
			G1	G2	G3	G4
Min. cost	1.456	0.518	0.45	0.36	0.22	0.25
Max. cost	1.514	0.641	0.36	0.36	0.21	0.23

Table 8. Optimal VAR allocation (Case 2-Scneraio 3)

Case	SVC bus number and VAR value								
	4	5	7	9	10	11	12	13	14
Min. cost	0.0	0.14	0.18	0.0	0.0	0.0	0.0	0.0	0.0
Max. cost	0.0	0.0	0.13	0.16	0.0	0.10	0.00	0.17	0.14

6. Conclusions

This study investigates the decision-making process of VAR sources for the long-term VAR planning problem with considering seasonal variations in wind power, solar PV, and load. To capture the seasonal variations of load and RES, their fluctuations have been represented using typical seasonal days constructed based on their historical seasonal data. The presented method highlights the trade-off between real expenses and the necessary level of system security, where two confining objective functions are optimized to achieve the lowest overall cost along with an appropriate VAR reserve that assures an acceptable security level for all anticipated conditions in the planning horizon. The proposed approach is solved by employing an integrated approach that incorporates conventional methods and the multi-objective genetic algorithm NSGA-II. The combination of the conventional method and NSGA-II allows to solve each simulated state individually and easily obtain the common optimal VAR allocation for all investigated states. The suggested technique has been implemented effectively on the IEEE 14-bus system. The computational results highlight the vital importance of employing the typical seasonal day representation to achieve the lowest cost while maintaining the necessary VAR reserve, which in turn allows for the achievement of an acceptable security level in emergency situations. The numerical results demonstrate that higher VAR reserve values require higher VAR installation expenses. Therefore, the system operator must achieve a fair balance between the planned VAR reserve and the associated VAR installation cost. Furthermore, simulation outcomes show that the suggested model can identify a set of Pareto optimal solutions, providing system planners the ability to conduct flexible analysis and reach an acceptable compromise between the investment cost, operating cost, and necessary VAR reserve for preserving voltage stability.

Further study can be conducted to establish a more computationally efficient solution strategy for the current computationally challenging problem by simplifying the stated formulation and carrying out an appropriate modification of the developed solution algorithm.

References

[1] N. Yorino, E. E. El-Araby, H. Sasaki and S. Harada, "A new formulation for FACTS allocation for security enhancement against voltage collapse", IEEE Trans. Power Systems, vol. 18, no. 1, pp. 3-10, Feb. 2003.

[2] N. Karmakar and B. Bhattacharyya, "Optimal reactive power planning in power transmission network using sensitivity based bi-level strategy", Sustainable Energy, Grids and Networks, vol. 23, 2020.

[3] Q. Nguyena, X. Kea, N. Samaana, J. Holzera, M.Elizondoa , H. Zhoua, Z. Houa, R. Huanga, M. Vallema, B. Vyakaranama, M. Ghosala, and Y. V. Makarova, "Transmission-distribution long-term volt-var planning considering reactive power support capability of distributed PV", International Journal of Electrical Power & Energy Systems, vol. 138, June 2022, 107955.

[4] R. Syah, P. Khorshidian Mianaei, M. Elveny, N. Ahmadian, D. Ramdan, R. Abibifar, and A. Davarpanah, "A new hybrid algorithm for multi-objective reactive power planning via facts devices and renewable wind resources", Sensors, 21(15), 2021, 5246. doi:10.3390/s21155246.

[5] T.A. Costa, W.G. Zvietcovich, F.R.A.C. Baracho, and L. J. S. Damião, "Optimal allocation of capacitors banks in radial distribution systems using clonal algorithm", in 2018 6th International Conference on Smart Grid (icSmartGrid), pp. 92-97,2018.

[6] N. Yang, C.W. Yu, F.S. Wen and C.Y Chung, "An investigation of reactive power planning based on chance constrained programming", International Journal of Electrical Power & Energy Systems. vol. 29, pp. 650–656, 2007.

[7] J. López, J. Contreras, and J. R. S. Mantovani, "Reactive power planning under conditional-value-at-risk assessment using chance-constrained optimization", IET Gener. Transm. Distrib., vol.9, no. 3, pp. 231-240, 2014.

[8] Y. Hong and K. Pen, "Optimal VAR planning considering intermittent wind power using Markove model and quantum evolutionary algorithm", IEEE Trans. Power Syst., vol. 25, no.4, pp. 2987–2996, 2010.

[9] M. Dadkhah and B. Venkatesh, "Cumulant based stochastic reactive power planning method for distribution systems with wind generators", IEEE Trans. Power Syst., vol 27, no. 4, pp. 2351–2359, 2012.

[10] H. Amaris and M. Alonso, "Coordinated reactive power management in power networks with wind turbines and FACTS devices", Energy Convers. Manag, vol 52, pp. 2575–2586, 2011.

[11] M. Alonso, H. Amaris, and C. Alvarez-Ortega, "A multiobjective approach for reactive power planning in networks with wind power generation", Renew. Energy, vol 37, pp. 180–191, 2012.

[12] M. Niu and Z.Y. Dong, "DE-based two-stage reactive power planning with wind power penetration", in 9th IET International Conference on Advances in Power System Control, Operation and Management, 2012. doi:10.1049/cp.2012.2151.

[13] A.E. and A. Eladl, "Planning of multi-type FACTS devices in restructured power systems with wind generation", International Journal of Electrical Power & Energy Systems, vol. 77, pp. 33–42, 2016. doi:10.1016/j.ijepes.2015.11.023.

[14] M. Niu and Z. Xu, "Reactive power planning for transmission grids with wind power penetration", Proc. Of IEEE PES ISGT Asia, May, 2012.

[15] X. Fang, F. Li, Y. Wei, R. Azim and Y. Xu, "Reactive power planning under high penetration of wind energy using Benders decomposition, " IET Gener. Transm. Distrib., vol. 9, no. 14, pp. 1835-1844, Nov. 2015.

[16] F. Ugranli and E. Karatepe, "Coordinated TCSC allocation and network reinforcements planning with wind power", IEEE Trans. Sustain. Energy, vol. 8, no. 4, pp. 1694-1705, Oct. 2017.

[17] N. Gupta, "Stochastic optimal reactive power planning and active power dispatch with large penetration of wind generation", Journal of Renewable and Sustainable Energy, vol. 10, no.2,2018, 025902. doi:10.1063/1.5010301.

[18] N. Savvopoulos, C.Y. Evrenosoglu, A. Marinakis, A. Oudalov, and N. Hatziargyriou, "A long-term reactive power planning framework for transmission grids with high shares of variable renewable generation", in IEEE Milan PowerTech, 2019. doi:10.1109/ptc.2019.8810680.

[19] N. Gupta, "Probabilistic optimal reactive power planning with onshore and offshore wind generation, EV, and PV uncertainties", IEEE Trans. Ind. Appl., vol.56, no. 4, pp. 4200-4213, 2020.

[20] J. Lopez, D. Pozo, J. Contreras, and J.R.S. Mantovani, "A multiobjective minimax regret robust VAr planning model", IEEE Transactions on Power Systems, vol. 32, no. 3, pp. 1761–1771, 2017. doi:10.1109/tpwrs.2016.2613544.

[21] Y. Chi, Y. Xu, and T. Ding, "Coordinated Var planning for voltage stability enhancement of a wind-energy power system considering multiple resilience indices", IEEE Transactions on Sustainable Energy, vol. 11, no. 4, pp. 2367-2379,2020.

[22] A.H. Shojaei, A.A. Ghadimi, M.R. Miveh, F. Mohammadi, and F. Jurado, "Multi-objective optimal reactive power planning under load demand and wind

power generation uncertainties using ε-constraint method", Applied Sciences, vol. 10, no. 8, 2020,2859.

[23] A.H. Shojaei, A.A. Ghadimi, M.R. Miveh., F.H. Gandoman, and A. Ahmadi", Multiobjective reactive power planning considering the uncertainties of wind farms and loads using Information Gap Decision Theory", Renewable Energy vol. 163, pp. 1427-1443, January 2021. doi:10.1016/j.renene.2020.06.129.

[24] Y. Chi, Y. Xu, and R. Zhang, "Many-objective robust optimization for dynamic var planning to enhance voltage stability of a wind-energy power system", IEEE Transactions on Power Delivery, vol. 36, no.1, pp. 30-42, Feb. 2021. doi:10.1109/tpwrd.2020.2982471.

[25] Y.M. Atwa, E.F. El-Saadany, M.M.A Salama, and R. Seethapathy, "Optimal renewable resources mix for distribution system energy loss minimization", IEEE Transactions on Power Systems, vol 25, no. 1, pp. 360–370, 2010 . doi:10.1109/tpwrs.2009.2030276.

[26] P. Kayal, and C.K. Chanda, "Optimal mix of solar and wind distributed generations considering performance improvement of electrical distribution network", Renewable Energy, vol. 75, pp. 173–186, 2015. doi:10.1016/j.renene.2014.10.003.

[27] N.S. Ghiasi, S.M.S. Ghiasi, and R. Hadidi, "Stochastic seasonal planning of DG-based smart grid and energy hub by considering demand response program and environmental impacts", in 2023 11th International Conference on Smart Grid (icSmartGrid), 2023.

[28] A. Ova and S. Demirbas, "Estimating wind power plant outputs in transmission system planning studies based on probability approaches", in 2021 10th International Conference on Renewable Energy Research and Applications (ICRERA), pp. 180-183, 2021.

[29] S. Sannigrahi, S.R. Ghatak, and P. Acharjee, "Multi-scenario based Bi-level coordinated planning of active distribution system under uncertain environment", IEEE Transactions on Industry Applications, vol. 56, no. 1., pp. 850-863, 2020.

[30] S.N.V.S.K. Chaitanya, R.A. Bakkiyaraj, B. V. Rao, and K. Jayanthi, "Scenario-based method to solve optimal reactive power dispatch using modified Ant Lion optimizer considering uncertainties in load, solar, and wind power", International Journal of Renewable Energy Research, vol 13, no.4, pp 279-291, 2023.

[31] M. Eghbal, N. Yorino, E. E. El-Araby and Y. Zoka, "Multi load level reactive power planning considering slow and fast var devices by means of particle swarm optimization", Proc. of IET Transaction on Generation, Transmission and Distribution, Vol. 2, no. 5, pp.743-751, 2008.

[32] E. E El-Araby and N. Yorino, "Reactive power reserve management tool for voltage stability enhancement", IET Generation, Transmission & Distribution, vol 12, no. 8, pp.1879–1888, 2018.

[33] K. Deb, A. Pratap, S. Agarwal, and T. Meyarivan, "A fast and elitist multiobjective genetic algorithm: NSGA-II", IEEE Trans. Evol. Comput., vol. 6, no. 2, pp. 182–197, Apr. 2002.

[34] M.K. Heris, NSGA-II in MATLAB (URL: https://yarpiz.com/56/ypea120-nsga2), Yarpiz, 2015. [Accessed:13 Oct.-2023]

[35] M.A. Kamarposhti, I. Colak, H. Shokouhandeh, C. Iwendi, S. Padmanaban, and S. S. Band, "Optimum operation management of microgrids with cost and environment pollution reduction approach considering uncertainty using multi-objective NSGAII algorithm", IET Renewable Power Generation, pp. 1-13, August 2022, doi.org/10.1049/rpg2.12579.

[36] P. Stackhouse, "Nasa power", Nasa.gov. [Online]. Available: http://power.larc.nasa.gov/data-access-viewer/. [Accessed:23 Oct.-2023]